

## Diagnosis Of Clay Minerals In Selected Areas Of Sulaymaniyah Governorate Using X-Ray Diffraction (Xrd) And Their Utilization In Sustainable Development

Shatha Hadi Mahmoud\* and Haleema A. Abdul rahman

Department of Soil Science and Water Resources, College of Agricultural Engineering Sciences, University of Baghdad, Iraq

\*corresponding author: [shatha.hadi2307p@coagri.uobaghdad.edu.iq](mailto:shatha.hadi2307p@coagri.uobaghdad.edu.iq)

### Abstract

The study of the mineralogical composition of the clay fraction is of great importance for understanding soil genesis and pedogenesis, assessing the degree of homogeneity of soil body materials, and characterizing soil-forming processes. The study area was selected in Sulaymaniyah Governorate, northern Iraq, between longitudes 35°49'89.113"–35°49'93.795" E and latitudes 45°47'84.917"–45°53'85.490" N, with a total area of 17.023 km<sup>2</sup>. Four areas were selected: Penjwin (471 km<sup>2</sup>), Said Sadiq (4731 km<sup>2</sup>), Sharazur (1801 km<sup>2</sup>), and Qaradagh (717 km<sup>2</sup>) for clay mineral identification. Three pedons were excavated in each area, giving a total of 12 pedons. Seven surface soil samples were also collected from each area. Sampling of soil samples was done at the study sites with precise study points being identified by use of a Global Positioning System (GPS). The purpose of this study was to establish the mineralogical composition of the soils. Physical and chemical tests were done, as well as mineralogical tests by X-ray diffraction (XRD). The results of X-ray diffraction, which were brought by the powder method to diagnose soil samples and identify the most predominant minerals, revealed that the most predominant minerals were 2:1: clay minerals and 1:1:2 clay minerals. Montmorillonite and chlorite were noted to dominate each other respectively. Chlorite prevailed in most instances over montmorillonite even though most of the soils examined were Vertisols with chestnut soils. The findings also revealed that there were two kinds of mica minerals, including dioctahedral mica (muscovite) and trioctahedral mica (biotite). Muscovite was prevailing because it was more resistant to weathering as compared to biotite. Other soils possessed quite high content of kaolinite that is not surprising because the soils are usually calcaeous and have alkaline reaction. The prevalence of kaolinite could be explained by the geological deposition in the regions.

Keywords: clay minerals, X-ray diffraction, kaolinite, chlorite, montmorillonite, muscovite.

### Introduction

Clay is a mineral that is naturally found in abundance and its specific physical and chemical characteristics have rendered it essential in most of the life dimensions (Ismail and Omar, 2014). Since ancient times, humans have used clay, which has been significant in many industries, such as ceramics, construction materials, healthcare, agriculture, civil engineering, environmental management, and chemical industries (Moreno-Maroto and Alonso-Azcarate, 2018; Ali et al., 2023).

Clay minerals are very instrumental in the nutrition of plants and a significant source of physical and chemical characteristics of soils, hence a key means through which plants can grow. There are also a number of techniques that can be used in determining the clay minerals in the soil among them being X-ray diffraction (XRD) which is the most common technique. These other techniques are: differential thermal analysis (DTA), transmission electron microscopy (TEM), and scanning electron microscopy (SEM). All these are methods employed in identification of clay minerals.

Clay minerals play a crucial role in agriculture and are a part of hydrated silicate of aluminum silicate group, phyllosilicates or layer silicates. These are typified by fine particle sizes that are less than 2  $\mu\text{m}$ . Out of the existing kinds of the clay minerals, the most significant ones are five and they include chlorite, illite, vermiculite, montmorillonite-smectite, and kaolinite (Dogan, 2009).

The clay minerals are significant to the soil chemistry as they impact on the movement and retention of the pollutants and metals. They also show a large ability to retain water and nutrients and this reflects on the availability of moisture in soil as well as nutrients to plants (Grim, 1962; Dogan, 2009).

X-ray diffraction (XRD) is a relevant method that is applied to determine minerals that cannot be detected through alternative methods. The procedure will entail the creation of X-rays in an X-ray tube which is then pointed at the sample. The X-rays that have diffracted are collected and recorded as both the sample and the detector rotate through the angles. It is this fundamental principle that underlies all methods of diffraction. In the process, as a mineral, a lattice plane has enough interplanar spacing (d-spacing) to disperse X-rays at a certain angle, denoted as  $\theta$ , the maximum intensity of the diffracted X-rays is obtained (Brady et al., 1995; Ismail and Omar, 2014). So, X-ray diffraction is used to obtain critical information on itemizing and characterizing minerals.

According to a study by Majied and Essa (2024) on X-ray diffraction analysis, the abundance of clay minerals was observed to follow order as: minerals of smectite type were present in higher proportions than mica/chlorite minerals and then layered clay

minerals, and then kaolinite. It was also found in the study that parent material, slope, topography, and distance between mountainous margins determine the preponderance of certain clay minerals in soils. These results add to the significance of geological and pedogenic factors in mineral composition of soils, as it has been demonstrated in earlier research on the importance of weathering processes and geographic difference in the determination of the soil properties.

### Research Methodology

In the Sulaymaniyah Governorate, four areas were chosen and they include Said Sadiq, Penjwin, Qaradagh and Sharazur as indicated in Figure 1.

There were a number of reconnaissance field trips, which were used to establish the location of sampling sites and determine them accurately with the help of a Global Positioning System (GPS).

In each area, three soil profiles were dug, which made a total of 12 profiles. Also, surface soil samples were collected in each area (6 surface samples), and the two surface samples were replicated in two neighboring areas.

Soil samples were collected from each pedon, including surface and subsurface horizons, along with an additional surface sample from each site, for mineral identification using X-ray diffraction (XRD).

Satellite imagery of the study areas was obtained, and RGB bands were extracted to calculate the Normalized Difference Vegetation Index (NDVI).

The results obtained from X-ray diffraction (XRD) analysis were interpreted.

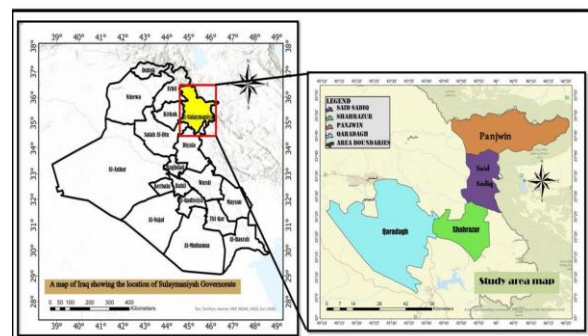
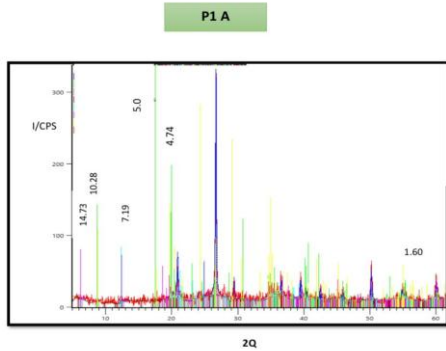


Figure 1 illustrates the study area.

**Results and Discussion**

The presence of the diffraction pattern and its measurement up to  $2\theta = 60^\circ$  aimed to reveal the sixth-order reflection at  $1.60 \text{ \AA}$ , which is characteristic of the mineral montmorillonite and allows its distinction from chlorite diffraction in the sample. This approach was adopted because the powder method was used for mineral identification instead of the casting method, as illustrated in Figure 2.



**Figure (2)** shows the presence of minerals in the first pedon of the surface horizon in the Said Sadiq area.

The results presented in Figure (3) for the subsurface

pedons P1C1, P2C1, and P3C1, as well as the surface pedons P7A and P8A, showed diffraction peaks at  $14.73 \text{ \AA}$  and its third-order reflection at  $4.74 \text{ \AA}$ , confirming the presence of chlorite in the examined samples. The appearance of the  $1.60 \text{ \AA}$  peak, which represents the sixth-order reflection of montmorillonite, indicates that part of the  $14.73 \text{ \AA}$  reflection corresponds to montmorillonite.

It should be noted that the samples were analyzed using the powder method, which made it difficult to confirm the above assumption. A clearer distinction between chlorite and montmorillonite could have been achieved using the casting method, where differentiation is possible through ethylene glycol saturation treatment.

Mica minerals were identified by the presence of a diffraction peak at  $10.07 \text{ \AA}$  and its second-order reflection at a basal spacing of  $5.00 \text{ \AA}$  with strong intensity, confirming the presence of dioctahedral mica (muscovite) in the examined samples.

Kaolinite was identified by the appearance of a diffraction peak at  $7.9 \text{ \AA}$ .

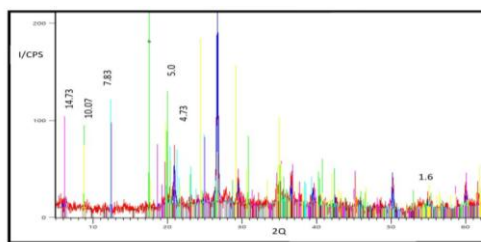
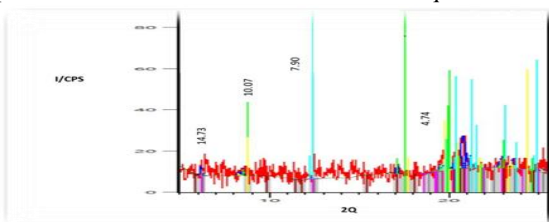


**Figure (3)** illustrates the presence of minerals in the first pedon of the subsurface horizons in the Said Sadiq area and in the

surface horizons of the Qaradagh area.

The results shown in Figure (4) for the surface pedon P2A and the subsurface pedon P12C1 revealed diffraction peaks at  $14.73 \text{ \AA}$  and its third-order reflection at  $4.74 \text{ \AA}$ , confirming the presence of chlorite in the examined samples. Mica minerals were identified by the appearance of a diffraction peak at  $10.07 \text{ \AA}$ .

**Figure (4)** shows the presence of minerals in the second pedon of the surface horizon in the Said Sadiq area



Kaolinite appeared at a basal spacing of  $7.90 \text{ \AA}$ . Notably, the intensity of its diffraction peak was high, indicating a relatively high

kaolinite content in the sample, despite the generally unfavorable conditions of Iraqi soils for kaolinite occurrence, as it typically forms under acidic soil conditions. The elevated kaolinite content in the examined clay soils may be attributed to earlier geological deposition processes.

The emergence of diffraction peaks at  $14.73 \text{ \AA}$ , and its third order reflection at  $4.74 \text{ \AA}$  as shown in Figure (5) of the third surface pedon P3A indicates the existence of chlorite in the sample under analysis.

The first-order peak at  $10.07 \text{ \AA}$  identified mica minerals, and the second-order one was weak at a basal spacing of  $5 \text{ \AA}$ , which proved the presence of mica minerals in trioctahed form (biotite). It is possible that the mineralogical studies explain the high content of biotite in the parent rocks attributed to its low weathering resistance in comparison to dioctahedral mica (muscovite)—the abundance of biotite in the soils under analysis (which is characteristic of the Iraqi soils) is explained by the abundance of biotite in the parent rocks (Essa, 2022; Al-Fatlawi, 2012; Al-Shahmani, 2020; Shahad, 2021).

A diffraction peak was found at  $7.90 \text{ \AA}$  to indicate kaolinite.

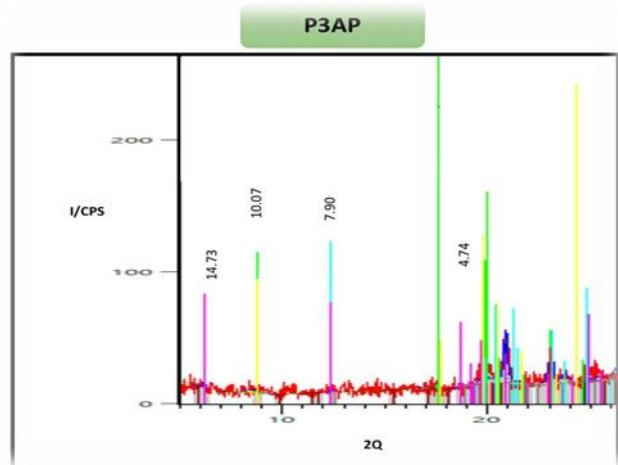


**Figure (5)** shows the presence of minerals in the third pedon of the surface horizon in the Said Sadiq area.

Figure (6) of the surface pedon P4A revealed a peak of diffraction to both the first and the second, third, and sixth-order reflection of basal spacings of  $7.08, 4.59$  and  $1.60$  at  $14.73 \text{ \AA}$ , which proves that montmorillonite was present in the sample.

Chlorite was identified by peaks at  $14.73 \text{ \AA}$  and its second and third-order reflections at  $7.08$  and  $4.74 \text{ \AA}$ , respectively. Mica minerals were detected with a first-order peak at  $10.04 \text{ \AA}$  and a second-order peak at  $5 \text{ \AA}$  with medium intensity, indicating the presence of both trioctahedral mica (biotite) and dioctahedral mica (muscovite).

Kaolinite was identified by its first-order peak at  $7.08 \text{ \AA}$  and second-order peak at  $3.57 \text{ \AA}$ . Additionally, a peak at  $24.54 \text{ \AA}$  was observed, representing the first-order reflection of a regular interstratified mineral, specifically mica-smectite (M-S).

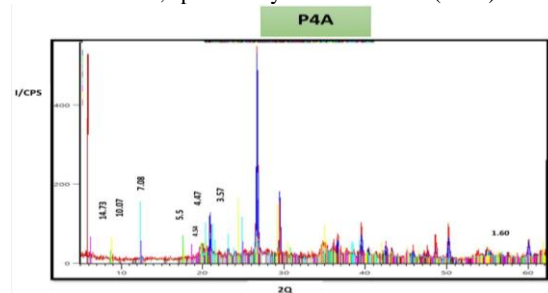


Figure (6) shows the presence of minerals in the fourth pedon of the surface horizon in the Penjwin area.

The results for pedon 1P4C of the subsurface horizon and pedon P5A of the surface horizon, shown in Figure (7), revealed

diffraction peaks at 14.73 Å and its second and sixth-order reflections at basal spacings of 7.19 and 1.60 Å, respectively, confirming the presence of montmorillonite in the sample.

Chlorite was identified by peaks at 14.73 Å and its second and third-order reflections at 7.19 and 4.74 Å, respectively.

Mica minerals were identified by the first-order peak at 10.40 Å and a strong second-order peak at 5 Å, confirming the presence of dioctahedral mica (muscovite) in the sample.

Kaolinite was detected by its first-order peak at 7.19 Å and a strong second-order peak at 3.57 Å.

Additionally, a peak at 24.5 Å represented the first-order reflection of a regular interstratified mineral, specifically mica-smectite (M-S).

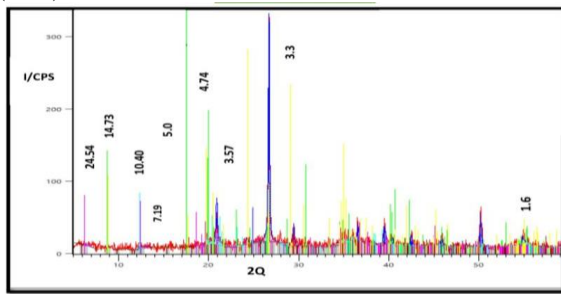
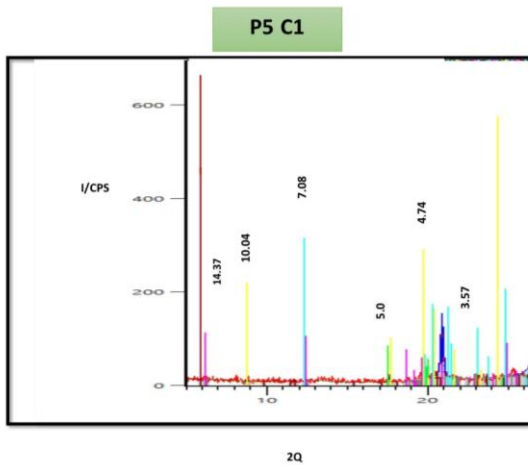


**Figure (7)** shows the presence of minerals in the fourth pedon of the subsurface horizon in the Penjwin area.

**Pedon P5C1**

The results in Figure (8) revealed diffraction peaks at 14.73 Å and its second and third-order reflections at basal spacings of 7.08 and 4.74 Å, confirming the presence of chlorite in the sample. Mica minerals were identified by a first-order peak at 10.04 Å and a medium-intensity second-order peak at 5 Å, indicating the presence of trioctahedral mica (biotite) and dioctahedral mica (muscovite). Kaolinite was detected by its first-order peak at 7.08 Å and second-order peak at 3.57 Å.

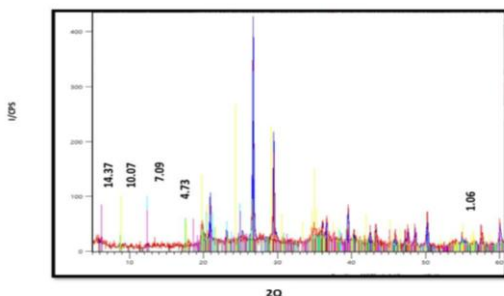


indicating the presence of trioctahedral mica (biotite) and dioctahedral mica (muscovite). Kaolinite was detected by its first-order peak at 7.08 Å and second-order peak at 3.57 Å.

**Figure (8)** shows the presence of minerals in the fifth pedon of the subsurface horizon in the Penjwin area.

**Pedon P6A**

The results for surface horizons P6A, P9A, P10A, P11A, P12A, and subsurface horizons P7C1, P8C1, P9C1, P10C1, P11C1 (Figure 9) revealed



diffraction peaks at 14.73 Å and its third-order reflection at 4.74 Å, confirming the presence of chlorite. The 1.60 Å peak, representing the sixth-order reflection of montmorillonite, indicated that part of the 14.73 Å reflection corresponds to montmorillonite. High intensity of the 14.73 Å peak suggests a high chlorite content, likely due to transformation of montmorillonite into chlorite, a process known as chloritization, common in chestnut soils such as those in the study area (Essa, 2022; Essa & Al-Watifi, 2022). Mica minerals were identified by a peak at 10.07 Å.

**Figure (9)** shows the presence of minerals in the sixth surface pedon in the Penjwin area.

**Pedon P6C1**

As shown in Figure (10), the diffraction peaks at 14.73 Å and its sixth-order reflection at 1.60 Å confirm the presence of montmorillonite. Mica was identified by a peak at 10.09 Å, with a strong second-order peak at 5 Å, indicating dioctahedral mica (muscovite). Kaolinite appeared at 7.9 Å.

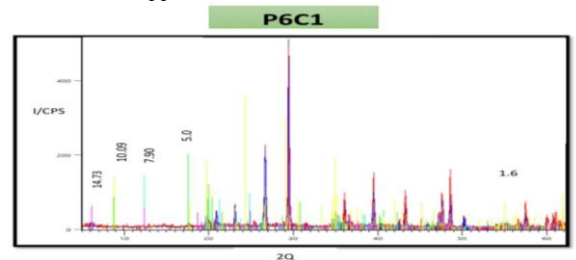


**Figure (10)** shows the presence of minerals in the sixth subsurface pedon in the Penjwin area.

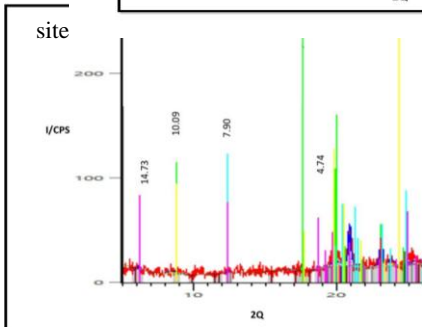
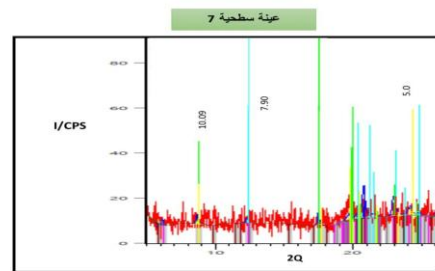
**Surface Samples 5 and 20**

Figure (11) shows peaks at 14.73 Å and its third-order reflection at 4.74 Å, confirming chlorite. Mica was identified at 10.09 Å. Kaolinite was not detected, consistent with the basic soil conditions and high exchangeable calcium content. The 7.90 Å peak represents the second-order reflection of chlorite.

**Figure (11)** shows the presence of minerals in the surface sample in the Said Sadiq area.

**Surface Sample 7**

Figure (12) shows diffraction peaks at 10.09 Å, its second-order at 5 Å, and third- and sixth-order reflections confirming the presence of mica. The strong second-order peak at 5 Å indicates dioctahedral mica (muscovite). The absence of 14 Å peaks (montmorillonite and chlorite) indicates minimal weathering at this



**Figure (12)** shows the presence of minerals in the surface sample in the Said Sadiq area.

**Surface Samples 10, 15, and 25**

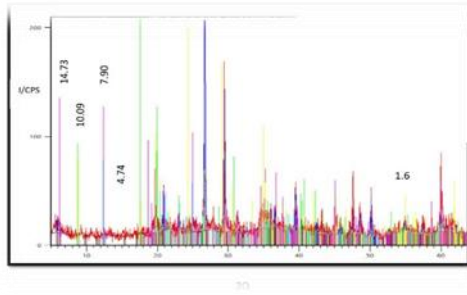


Figure (13) shows peaks at 14.73 Å and its third-order reflection at 4.74 Å, confirming chlorite.

The 1.60 Å peak indicates montmorillonite, suggesting part of the 14.73 Å peak corresponds to montmorillonite. High intensity of the 14.73 Å peak reflects high chlorite content, likely due to montmorillonite transformation during chloritization. Mica was identified by a peak at 10.09 Å.

Figure (13) shows the presence of minerals in surface samples in the Sharazur area.

### Remote Sensing

Satellite imagery of the study areas was obtained, and RGB bands were extracted to calculate NDVI, indicating soil use for agriculture (Figure 14).

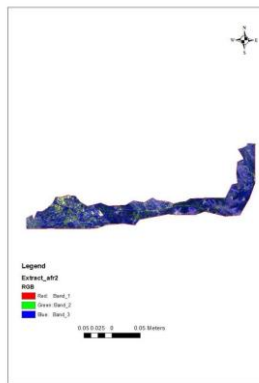


Figure 14: Satellite imagery and NDVI map of the study areas for assessing vegetation cover and agricultural potential.

### Sustainable Development

NDVI analysis was done in order to connect the soil mineral with agricultural activity. The values of NDVI were between 0.222 and 0.627, which means that all study regions have adequate vegetable covers and most of them can be exploited in agriculture (Figure 15). The four regions differed on the agricultural use, with low and high values of NDVI.

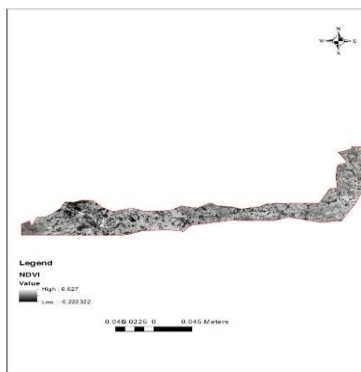


Figure 15: NDVI distribution of the study areas indicating suitability for sustainable agricultural use.

### Conclusion

The findings show that there is an evident difference in minerals in the Said Sadiq and Penjwin region whereas in Sharazur and Qaradagh, there existed relative similarity in the mineral composition and type. Such similarity can be attributed to little or insignificant weathering or rather the impact of geological and pedogenic environments which determine mineral composition of soil. These results can be compared with the past research done on the influence of weathering and geographic variation on defining soil properties.

### Acknowledgments

The authors acknowledge the sincere gratitude to all the researchers and colleagues that took part in this research. A special mention is given to the professor under whom this paper was prepared as there was constant guidance and encouragement. The authors further credit the Department of Soil Science and Water Resources and the College of Agricultural Engineering Sciences, University of Baghdad with the provision of the facilities and resources that it used to undertake this research.

### References

- Ali, M.H., Abood, M.R. and Zarraq, G.A. 2023. Validity of the Injana claystones as fillers. *Iraqi Geological Journal* 56(1A):42–49. <https://doi.org/10.46717/igj.56.1A.5ms-2023-1-17>
- Brady, J.B., Newton, R.M. and Boardman, S.J. 1995. New uses for powder X-ray diffraction experiments in the undergraduate curriculum. *Journal of Geological Education* 43(5):466–470. DOI: <https://doi.org/10.5408/0022-1368-43.5.466>
- Dogan, H.M. 2009. Mineral composite assessment of the Kelkit River Basin in Turkey by means of remote sensing. *Journal of Earth System Science* 118:701–710. DOI: <https://doi.org/10.1007/s12040-009-0059-9>
- Grim, R.E. 1962. Applied clay mineralogy. رابط تحميل كتاب <https://www.geokniga.org/bookfiles/geokniga-applied-clay-mineralogy.pdf>
- Ismail, N.R. and Omar, H.M. 2014. Assessment of some clay deposits from Fatha Formation (Middle Miocene) for brick manufacturing in Koya Area, Northern Iraq. *Aro – The Scientific Journal of Koya University* 2(1):16–23. <https://aro.koyauniversity.org/index.php/aro/article/view/12>
- Jassim, S.Z. and Goff, J.C. 2006. *Geology of Iraq*. Dolin, Sro. Distributed by the Geological Society of London.: <https://www.geolsoc.org.uk/IRAQ>
- Majied, S.S. and Essa, S.K. 2024. The effect of different parent materials and topography on the mineral properties of some soils in Sulaymaniyah Governorate. *IOP Conference Series: Earth and Environmental Science* 1371:082017. DOI: <https://doi.org/10.1088/1755-1315/1371/8/082017>
- Moreno-Maroto, J.M. and Alonso-Azcárate, J. 2018. What is clay? A new definition of clay based on plasticity and its impact on soil classification systems. *Applied Clay Science* 161:57–63. DOI: <https://doi.org/10.1016/j.clay.2018.02.017>
- Zhang, Y., Pu, S., Li, R.Y.M. and Zhang, J. 2020. Microscopic and mechanical properties of undisturbed and remoulded red clay from Guiyang, China. *Scientific Reports* 10(1):18003. DOI: <https://doi.org/10.1038/s41598-020-74907-1>